DOE effect on BER performance in MSK space uplink chaotic optical communication

Mi Li (李 密)*, Yuan Chen (陈 媛), Yuejiang Song (宋跃江), Cheng Zeng (曾 丞), and Xuping Zhang (张旭苹)

Key Laboratory of Intelligent Optical Sensing and Manipulation, College of Engineering and Applied Sciences, Nanjing University, Nanjing 210093, China

**Corresponding author: limi@nju.edu.cn*

Received March 3, 2020; accepted April 16, 2020; posted online May 22, 2020

With the increasing demand for space optical communication security, space chaotic optical communication has attracted a great amount of attention. Compared with traditional space optical communication, a chaotic optical communication system has a higher bit error rate (BER) for its complex system design. In order to decrease the BER of space chaotic optical communication systems, we introduce two diffractive optical elements (DOEs) at a transmitting terminal (Tx). That is because the commonly used reflective optical antenna at Tx blocks the central part of the transmission beam, which leads to a great amount of power consumption. Introducing the DOEs into the optical subsystem at Tx can reshape the transmission beam from a Gaussian distribution to a hollow Gaussian distribution so that the block of the secondary mirror in the reflective optical antenna can be avoided. In terms of the DOE influence on communication quality, we give a BER model based on a minimum-shift-key (MSK) space uplink chaotic optical communication system to describe the DOE function. Based on the model, we further investigate the effect of the DOEs through analyzing the BER relationship versus basic system parameters based on the BER model. Both different mismatch conditions of chaotic systems and different atmospheric turbulence conditions are considered. These results will be helpful for the scheme design of space uplink chaotic optical communication systems.

Keywords: chaotic-encrypted communication; space uplink optical communication; atmospheric turbulence effects; diffractive optical element design; minimum-shift-key; bit error rate.

doi: 10.3788/COL202018.070601.

Free-space optical communication has developed for several decades and shows a good communication performance as many key technologies have been further enhanced[1,2]. However, with the demand for information security increasing, traditional space optical communication systems cannot satisfy communication safety standards because of the risk of being a target of eavesdropping. Different encryption technologies have been applied to space optical communication. Among them, the chaotic encryption method has earned great attention for its advantages of low attenuation and high bandwidth of optical devices and good anti-interference ability[3–5]. A fiber chaotic optical communication experiment over 120 km was carried out successfully in Athens in 2005[6].

In space chaotic optical communication systems, synchronous chaotic carriers are generated by controlling the design of chaotic circuits at the transmitting/receiving terminal (Tx/Rx). Randomly chaotic carriers are used to realize encryption at Tx and realize decryption through carrier cancellation at Rx[7,8]. The chaotic carrier is decided by the hardware design and the parameter design of the chaotic circuit at Rx must be completely the same as that at Tx, and then the communication security of the space chaotic optical communication is guaranteed. However, the bit error rate (BER) of space chaotic optical communication is much higher than that of traditional space optical communication for a relatively complex system design. In 2002, a 5 km free-space chaotic optical communication system was reported with a BER around 10^{-2}[9], which is hard for realizing high quality communication. In addition, high BER limits the increase of bit rate in space chaotic optical communication.

As BER and bit rate are two important measuring parameters in the space optical communication field[10], we must purchase methods to improve the BER performance of space chaotic optical communication. In our former investigation, we find that the transmission power will be consumed during the expanding process. The secondary mirror of the optical antenna blocks the central part of the Gaussian beam[11–13]. A couple of diffractive optical elements (DOEs) can be used to solve this problem[14,15]. They can reshape the Gaussian beam into a hollow Gaussian beam before it enters the optical antenna. So the practical transmission power at the exiting pupil will be enhanced and the transmission efficiency can theoretically be higher than 99% after introducing the DOEs[14].

In this Letter, we focus on the investigation of the DOE effect on the BER performance in a minimum-shift-key (MSK) space chaotic optical communication. Both atmospheric turbulence effects in the transmission channel and mismatch in the chaotic system are considered. We want to figure out whether introducing the DOEs can help the BER improvement and the optimization of the system design. These results will be helpful in engineering.

The system schematic of a space uplink chaotic optical communication system is shown in Fig. 1(a),

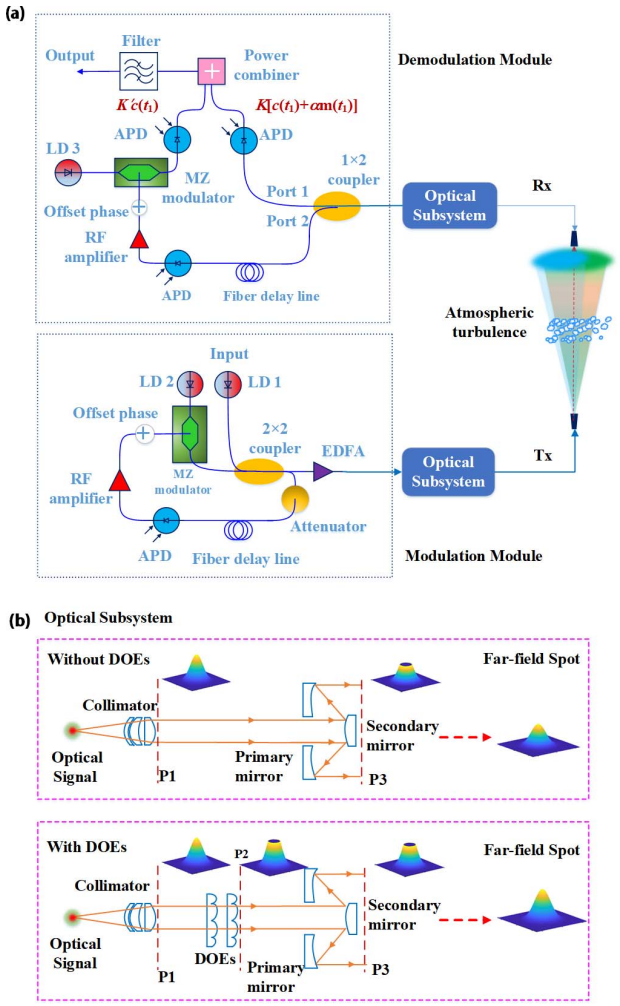

Fig. 1. (a) Schematic diagram of a space uplink chaotic communication system. (b) The optical subsystem before and after introducing the DOEs.

which includes a transmitting/receiving terminal and a transmitting channel. The transmitting/receiving terminal is composed of a chaotic modulation/demodulation circuit and an optical subsystem. The randomly chaotic carrier is generated by a Mach–Zehnder modulator. The fiber delay line is used to control the time delay to keep the chaotic carrier at Rx and Tx totally synchronized[16]. The signal wave will be separated from the carrier by a power combiner and then filtered. Figure 1(b) gives the detailed schematic of the optical subsystems at Tx. One is the traditional optical subsystem and the other is the improved structure after introducing the DOEs. The DOEs are placed in front of the optical antenna.

From Fig. 1(b) we can see that the central part of the Gaussian beam will be blocked by the secondary mirror of the optical antenna. A large part of the energy is lost, and the amplitude at the exiting pupil (P3) is A_{30}[14]:

$$A_{30}=\begin{cases} e^{-\frac{r_3^2}{w_{03}^2}} & r_{30}<|r_3|<r_{3m}, \\ 0 & \text{otherwise} \end{cases} \tag{1}$$

where r_{3m} and r_{30} are the radius of the exiting pupil and the secondary mirror, respectively, and ω_{03} is the waist at the exiting pupil. The power in the system without DOEs at P3 is E_{30}.

After introducing the DOEs, the input spot will be reshaped from a Gaussian distribution into a hollow Gaussian distribution with no power consumption. According to Ref. [14], the amplitude of the reshaped beam is marked as A_{31}:

$$A_{31}=\begin{cases} \sqrt{\frac{\alpha\cdot E_0}{E_{30}}}\cdot e^{-\frac{r_3^2}{w_{03}^2}} & r_{30}<|r_3|<r_{3m}, \\ 0 & \text{otherwise} \end{cases} \tag{2}$$

where α is the coefficient caused by the DOEs[17,18] and E_0 is the beam power at P1.

The far-field propagation process follows the Fraunhofer distribution principle[19] and, according to Ref. [14], the intensities before and after introducing the DOEs at Rx are marked as I_4:

$$I_4(x_4,y_4)=\begin{cases} (\frac{1}{\lambda L})^2\cdot|\mathcal{F}\{A_{30}(x_{30},y_{30})\}|^2 \text{ without DOE} \\ (\frac{1}{\lambda L})^2\cdot|\mathcal{F}\{A_{31}(x_{31},y_{31})\}|^2 \text{ with DOE} \end{cases}, \tag{3}$$

where λ is the wavelength and L is the transmission distance.

In space uplink optical communication systems, atmospheric turbulence will affect the transmission beam and lead to intensity fluctuations and beam wander. For an atmosphere that is changing with time, we use the probability density function (PDF) to describe the receiving intensity I under atmospheric turbulence effects[20]. The PDFs of the receiving intensity under the effects of intensity scintillation and beam wander are[21]

$$P_I(r,I)=\frac{1}{\sqrt{2\pi\sigma_I^2(r,L)}}\frac{1}{I}\cdot\exp\left\{-\frac{\left[\ln\frac{I}{\frac{1}{2}\int_{-R}^{R}\int_{-R}^{R}I_4(x_4,y_4)\mathrm{d}x_4\mathrm{d}y_4}+\frac{2r^2}{W^2}+\frac{\sigma_I^2(r,L)}{2}\right]^2}{2\sigma_I^2(r,L)}\right\}, \tag{4}$$

$$P(r)=\frac{r}{\sigma_r^2}\exp\left(-\frac{r^2}{2\sigma_r^2}\right), \tag{5}$$

where $\sigma_I^2(r,L)$ and σ_r^2 are the variance of intensity scintillation and beam wander, respectively, W and R are the spot radius and receiving diameter at Rx, and r is the offset between the receiving point and the beam center.

According to Ref. [22], for an avalanche photodiode (APD) detector, the noise variance and the signal value are

$$\sigma_1^2=\sigma_{d1}^2+\sigma_{d1}'^2+\sigma_n^2, \tag{6}$$

$$\sigma_0^2 = \sigma_{d0}^2 + \sigma_{d0}'^2 + \sigma_n^2, \tag{7}$$

$$m_1 = Ge(K_b + K_s) + 2I_{\mathrm{dc}}T_s, \tag{8}$$

$$m_0 = GeK_b + 2I_{\mathrm{dc}}T_s, \tag{9}$$

where $\sigma_{d1}^2 = (Ge)^2FK_{s11} + \sigma_T^2$, $\sigma_{d0}^2 = (Ge)^2FK_{s10} + \sigma_T^2$ and $\sigma_{d1}'^2 = (Ge)^2FK_{s21} + \sigma_T^2$, $\sigma_{d0}'^2 = (Ge)^2FK_{s20} + \sigma_T^2$ are the detective noise variances of APD1 and APD2 at signals 1 and 0. G is the gain of the photomultiplier, e is the electronic constant, and F is the excess noise factor. K_{s11}, K_{s21}, K_{s10}, and K_{s20} are the photon numbers of the two APDs at signals 1 and 0. σ_T^2 is the hot noise. σ_n^2 is mismatch noise variance $\sigma_n^2 = 1/2K^2\sigma_m^2$ [23], K is the amplitude of the output electrical signal of APD1, σ_m^2 is the chaotic mismatch level we define, and K_b and K_s are the photon numbers of the background light and signal light.

So, we give the BER of an MSK modulation module in chaotic optical communication based on Ref. [22]

$$\mathrm{BER_{DCD}} = \frac{1}{4}\left[\mathrm{erfc}\left(\frac{m_0 + a}{2\sqrt{2}\sigma_1}\right) + \mathrm{erfc}\left(\frac{m_0 - a}{2\sqrt{2}\sigma_1}\right)\right], \tag{10}$$

where $a = GeK_s$.

Taking atmospheric turbulence into consideration, we calculate the ensemble average of the BER at all values of the receiving intensity I as the actual BER. Thus, the ensemble average BER of an MSK space chaotic optical communication system can be expressed as

$$\mathrm{BER} = \int_0^\infty \int_0^\infty \mathrm{BER_{DCD}} \cdot \frac{1}{\sqrt{2\pi\sigma_I^2(r,L)}} \cdot \frac{1}{I}\frac{r}{\sigma_r^2}\exp\left(-\frac{r^2}{2\sigma_r^2}\right) \cdot \exp\left\{-\frac{\left[\ln\frac{2I}{\int_{-R}^{R}\int_{-R}^{R} I_4(x_4,y_4)\mathrm{d}x_4\mathrm{d}y_4} + \frac{2r^2}{W^2} + \frac{\sigma_I^2(r,L)}{2}\right]^2}{2\sigma_I^2(r,L)}\right\}\mathrm{d}r\mathrm{d}I. \tag{11}$$

In numerical simulation, the parameters in the space uplink chaotic optical communication system are set as shown in Table 1 [24,25]. The loss coefficient of the DOEs is caused by the insertion loss and diffraction loss of the DOEs. It should be noted that the chaotic signal will be amplified by the erbium-doped fiber amplifier (EDFA) at Tx, and at Rx the receiving power will be detected by the APDs with bandwidths larger than 1 GHz. Since the performance of these two key devices has been greatly improved in recent years, many good companies can be selected. For example, the EDFA (series of CEFA-C-PB-HP-CPB42) made by Keopsys company and the photodetector (RIP1-JJAF) made by Siletz company are all good choices. The atmospheric turbulence model is based on the Hufnagel–Valley model [26].

We show the intensity distribution at Tx/Rx in Fig. 2. Figure 2(a) is the intensity distribution of the input power. The input power will be expanded by the optical antenna and in this Letter the beam radius will be expanded by 4 times. The intensity distribution of the spot at the exiting pupil (P3) is shown in Figs. 2(b) and 2(c). The DOEs realize beam reshaping through changing the phase information of every point. We can see that the DOEs only improve the beam intensity while not influencing the beam profile at Tx. Thus, introducing the DOEs will not change the far-field propagation process. According to the Fraunhofer diffraction principle, the hollow Gaussian spot turns into a Gaussian-like spot. The intensity at Rx in the system with and without the DOEs is shown in Fig. 2(d). The peak value of the intensity can be enhanced by around 1.5 times after introducing the DOEs. The far-field spot radii in the system with and without the DOEs are the same, as the transmitting spot profile is not changed.

Table 1. Basic Parameter Values in the Space Uplink Chaotic Optical Communication System

Basic Parameter	Value
Height of ground station h_0	100 m
Height of satellite orbit H	45,000 km
Transmission power P_t	10 W
Transmission aperture W_o	0.08 m
Receiving diameter D_r	1 m
Zenith angle ζ	0°
Wavelength λ	1550 nm
Bit rate	1 Gbps
APD bandwidth	1 GHz
Expanding coefficient M	4
Loss coefficient of the DOEs	3%
Strong/weak atmospheric refractive index C_n^2	$\sim 10^{-12}/10^{-14}$

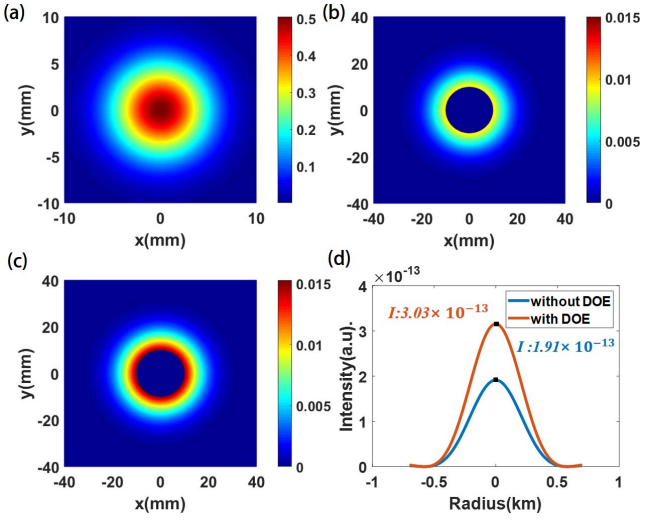

Fig. 2. (a) Input spot. (b) The spot at the exiting pupil in a system without the DOEs. (c) The spot at the exiting pupil in a system with the DOEs. (d) The intensity of the beam at Rx.

For a space uplink chaotic optical communication system, both atmospheric turbulence effects and system noises affect the communication quality. Based on the BER model derived above, we investigate the effect of the DOEs through analyzing the BER relationship with basic parameters. As the transmission power is the most direct parameter that can influence the BER, we first show the BER relationship curve versus transmission power under weak atmospheric turbulence in Fig. 3(a). In this case, we can see that the BER decreases with the increase of transmission power. Introducing the DOEs can also achieve this goal, as the substantial function of DOEs is to supplement the lost transmission power caused by the optical antenna. For a fixed obscuration ratio $(1/M)$, the larger the transmission power is, the more power the DOEs can complement. We can see that the DOEs can decrease the BER by more than 10^{-1} magnitude at $P_t = 10$ W. The mismatch level at Tx/Rx in a chaotic optical communication also influences the BER. In order to better explain the influence of the DOEs, we investigate the BER at different chaotic mismatch levels. In our simulation, we take a mismatch level higher than 10^{-1} as a large chaotic mismatch and that lower than 10^{-2} as a small chaotic mismatch. We can find that in a condition of weak atmospheric turbulence, the effect of the DOEs on the BER is more obvious at a small chaotic mismatch than that at a large chaotic mismatch.

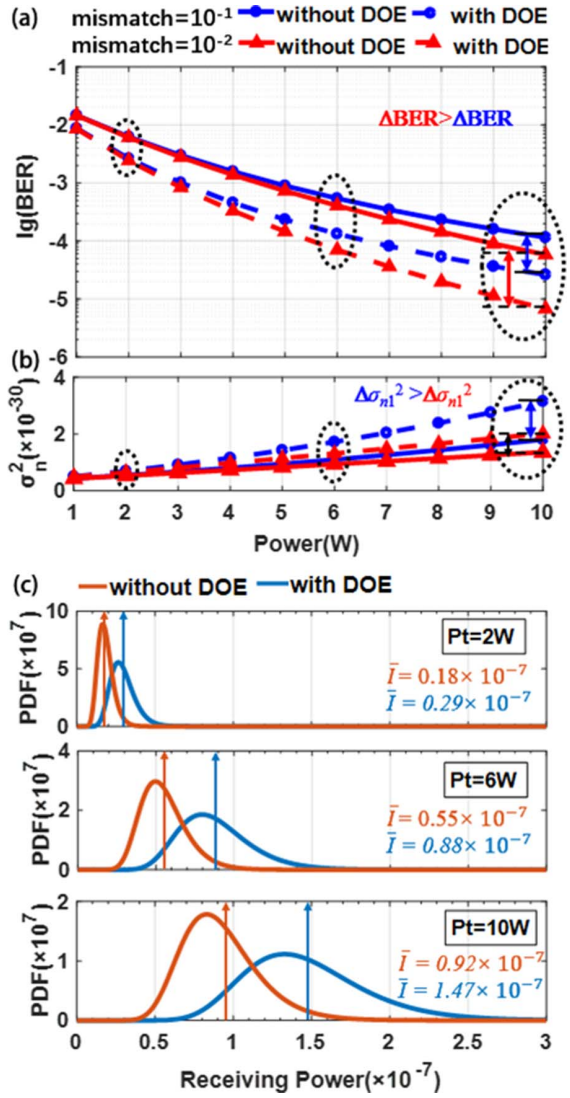

Fig. 3. Weak atmospheric turbulence. (a) The BER relationship versus transmission power at different chaotic mismatch levels. (b) The total noise relationship versus transmission power at different chaotic mismatch levels. (c) The PDF distribution at $P_t = 2$ W, 6 W, and 10 W. The $\bar{I}$ in red is the average receiving power in the system without the DOEs and the $\bar{I}$ in blue is the average receiving power in the system with the DOEs.

In order to make the explanation of the phenomenon clear, we give a further analysis from the perspective of the signal-to-noise ratio of the system. In space chaotic optical communication systems, the signal-to-noise ratio is often defined as $r = m_1/\sqrt{\sigma_1^2}$[27], where m_1 is the signal value and σ_1^2 is the noise variance of signal 1. Chaotic noise can be written as $\sigma_n^2 = 1/2K^2\sigma_m^2$, where the chaotic mismatch at a large chaotic mismatch is $\sigma_{\text{mlarge}}^2 = 0.1$, and the chaotic mismatch at a small chaotic mismatch is $\sigma_{\text{msmall}}^2 = 0.01$. Taking Eq. (6) and Eq. (8) and the expression of chaotic noise $\sigma_n^2 = 1/2K^2\sigma_m^2$ into the expression of the signal-to-noise ratio r, we can further give the signal-to-noise ratio r_{large} at a large chaotic mismatch condition and r_{small} at a small chaotic mismatch condition as

$$r_{\text{large}} = \frac{m_1}{\sqrt{\sigma_{d1}^2 + \sigma_{d1}'^2 + 1/2K^2\sigma_{\text{mlarge}}^2}}, \tag{12}$$

$$r_{\text{small}} = \frac{m_1}{\sqrt{\sigma_{d1}^2 + \sigma_{d1}'^2 + 0.1 \cdot (1/2K^2\sigma_{\text{mlarge}}^2)}}, \tag{13}$$

where σ_{d1}^2 and $\sigma_{d1}'^2$ are the noise variances of APD1 and APD2, and $1/2K^2\sigma_{\text{mlarge}}^2$ and $0.1 \cdot (1/2K^2\sigma_{\text{mlarge}}^2)$ are the chaotic noise variances at large and small chaotic mismatch conditions.

For the effect of the DOEs on the BER, we know that the DOEs will improve the receiving power at Rx. According to the analysis above, when the increment of the receiving power is the same, the increment of the signal value m_1 and the increment of the two APD noise values $(\sigma_{d1}^2 + \sigma_{d1}'^2)$ are the same. So, based on Eq. (12) and Eq. (13), the only difference lies in the mismatch noise, and the increment of the mismatch noise at a small mismatch level is only one-tenth of that at a large mismatch level. In this way, with the receiving power increasing, the improvement of the signal-to-noise ratio at a small mismatch noise will be better than that at a large mismatch noise. Here, in Fig. 3(b), we give the relationship curves of the total noise versus the transmission power at two mismatch levels. It shows clearly that the increment of the total noise caused by the DOEs is smaller at a small chaotic mismatch. So, in conditions of weak atmospheric turbulence, the effect of the DOEs on the BER is more obvious at a small chaotic mismatch than that at a large chaotic mismatch.

In Fig. 3(a) we also find that introducing the DOEs can decrease the BER more at a large transmission power. To explain the results more clearly, we further analyze the PDF of the receiving power. The transmission beam will be influenced by atmospheric turbulence effects like the intensity fluctuation and the beam wander in space uplink optical communication; the receiving power is floating, and the PDF model can describe the distribution of receiving power clearly. Figure 3(c) gives the PDF of the receiving power in the system with and without the DOEs at $P_t = 2$ W, 6 W, and 10 W. It shows that the PDF of the receiving power tends to shift to the right and be more centered on a large receiving power after introducing the DOEs or increasing the transmission power. Considering that the integral PDF curve is not specific enough, we use the average receiving power to analyze it further. It is clear that the PDF of the average receiving power will change to a δ function because the average receiving power is a fixed value. So, we marked the PDF of the average receiving power as a δ function in Fig. 3(c). We can see that the right-shift values of the average receiving power are 1.1×10^{-8}, 3.3×10^{-8}, and 5.5×10^{-8} at $P_t = 2$ W, 6 W, and 10 W after introducing the DOEs. It indicates that the right-shift of the average receiving power caused by the DOEs increases with the increase of the transmission power. That also explains why introducing the DOEs can decrease the BER more at a large transmission power in Fig. 3(a).

However, in extreme weather conditions or regions, the communication system will be affected by strong atmospheric turbulence. In this case, we change the near-ground atmospheric refractive index coefficient C_n^2 to 10^{-12} according to the Hufnagel–Valley atmospheric turbulence model[24]. As shown in Fig. 4(a), the overall system BER under strong atmospheric turbulence effects is higher than 10^{-4}. In this condition, the DOEs still work, though they will not perform as well as that under weak atmospheric turbulence. We can see that the DOEs can decrease the BER by about $10^{-0.6}$ magnitude at $P_t = 10$ W and mismatch level $= 10^{-2}$. Since the communication performance of the chaotic system is poor under strong atmospheric turbulence effects, we want to figure out whether the DOEs can help the BER below 10^{-3}. It shows that the required transmission power can decrease from about 9 W to 6 W after introducing the DOEs to keep the BER lower than 10^{-3}. Figure 4(c) can give a clearer explanation for these results, which shows the PDF of the receiving power at $P_t = 2$ W, 6 W, and 10 W under strong atmospheric turbulence effects. Compared with Fig. 3(c), we can see that the right-shift of the PDF caused by the DOEs under strong atmospheric turbulence is smaller than that under weak atmospheric turbulence when other conditions are the same. Taking $P_t = 10$ W as an example, the enhancement of the average receiving power is 5.5×10^{-8} W under weak atmospheric turbulence while the enhancement will only be 3.7×10^{-8} W under strong atmospheric turbulence. The changing trends of the receiving power at $P_t = 2$ W and $P_t = 6$ W are the same.

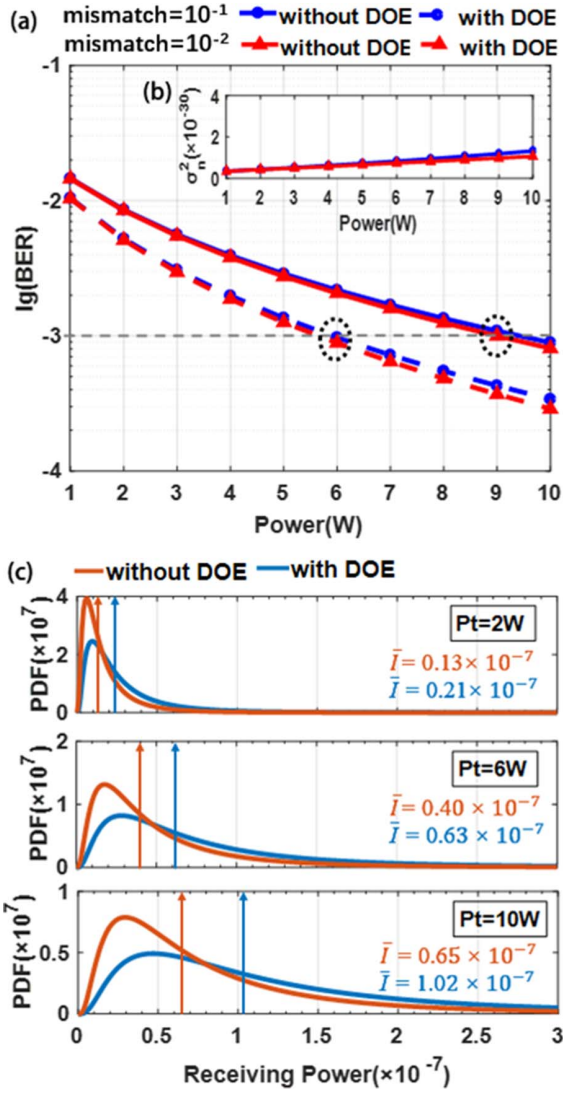

Fig. 4. Strong atmospheric turbulence. (a) The BER relationship versus transmission power at different chaotic mismatch levels. (b) The total noise relationship versus transmission power at different chaotic mismatch levels in a system without the DOEs. (c) The PDF distribution at $P_t = 2$ W, 6 W, and 10 W. The $\bar{I}$ in red is the average receiving power in the system without the DOEs and the $\bar{I}$ in blue is the average receiving power in the system with the DOEs.

This explains why the improvement of the DOEs on the BER in conditions of strong atmospheric turbulence is smaller than that in conditions of weak atmospheric turbulence.

Figure 4(a) also indicates that the influence of a chaotic mismatch is smaller under strong atmospheric turbulence effects than that under weak atmospheric turbulence effects. The conclusion is obvious, and we can also explain it from the perspective of signal and noise. For the signal-to-noise ratio $r = m_1/\sqrt{\sigma_1^2}$[27], a decreasing mismatch does not affect the signal value m_1. For the total noise σ_1^2, which is composed of the noise of APD1 and APD2, and the chaotic noise, a decreasing mismatch also does not affect the

noise of APD1 and APD2. So, we just need to further analyze the improvement of the chaotic noise here.

Based on the chaotic noise variance expression, $\sigma_n^2 = 1/2K^2\sigma_m^2$, we can give the improvement of the mismatch noise $\Delta\sigma_n^2$ when the mismatch level σ_m^2 decreases from 10^{-1} to 10^{-2} magnitude:

$$\Delta\sigma_n^2 = \frac{1}{2}K^2 \cdot 0.1 - \frac{1}{2}K^2 \cdot 0.01 = 0.09 \cdot \frac{1}{2}K^2, \qquad (14)$$

where K is the amplitude of the output electrical signal of APD1, which is proportional to the receiving power.

Considering that K is proportional to the receiving power, the improvement of the mismatch noise $\Delta\sigma_n^2$ is proportional to the square of the receiving power. As we know, the receiving power under a strong atmospheric turbulence is much smaller than that under a weak atmospheric turbulence. So, in conditions of strong atmospheric turbulence, the improvement of the mismatch noise $\Delta\sigma_n^2$ caused by a decreasing mismatch level will be not obvious. In addition, the noise of APD1 and APD2 are not affected by the decreasing mismatch mentioned above, and the improvement of the total noise caused by a decreasing mismatch level will also not be obvious. In Fig. 4(b), we give the relationship curves of the total noise versus power at two mismatch levels in the system without the DOEs under strong atmospheric turbulence. It shows clearly that the improvement of the total noise is not obvious when decreasing the mismatch level from 10^{-1} to 10^{-2} in strong atmospheric turbulence conditions. Considering that the signal is not affected by a decreasing mismatch, based on the expression of the signal-to-noise ratio r, the improvement on the signal-to-noise ratio will also not be obvious by decreasing the mismatch level. Thus, decreasing the mismatch level is not very helpful for the system BER improvement in strong atmospheric turbulence conditions.

We have analyzed the effect of DOE on BER improvement at different transmission powers in weak and strong atmospheric turbulence channels. Then, in order to understand the effect of DOE on optimization of the design of the practical system, we further analyze the relationship of the DOE effect on the BER versus other basic parameters based on Table 1. Since a low chaotic mismatch can decrease the BER and the mismatch of the chaotic system can be controlled below 10^{-2} by the electronic equipment nowadays, we investigate the BER relationship with other basic parameters in this condition. According to the analysis above, the DOEs influence the BER through changing the receiving power. However, after far-field propagation, the spot is very large and not all the transmission power can be achieved by Rx. How much power can be detected at Rx is decided by the receiving diameter. So, we analyze the relationship between the BER and receiving diameter. In Fig. 5, we can see that the BER decreases with the increase of the receiving diameter. That is because increasing the receiving diameter results in a large input signal in the APD. We can also find that the effect of the DOEs on

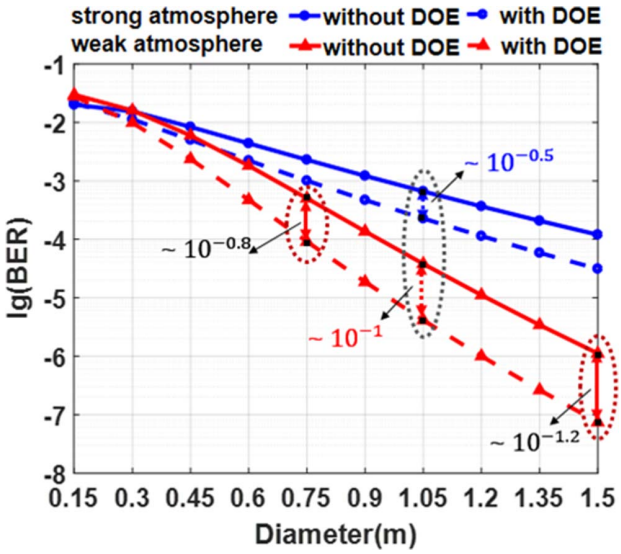

Fig. 5. BER relationship versus the receiving diameter at different atmospheric turbulence conditions.

the BER is more obvious at a large receiving diameter under weak atmospheric turbulence. For example, the BER decreases by $10^{-0.8}$ at $D_r = 0.75$ m while it decreases by $10^{-1.2}$ at $D_r = 1.5$ m after introducing the DOEs in this case. That is because the DOEs can improve the receiving power at a large receiving diameter. We have found that the improvement of the DOEs on the receiving power will be better at a large transmission power. The affect of increasing the receiving diameter on the receiving power is equivalent to that of increasing the transmission power at a fixed receiving diameter. So the function of the DOEs at a large receiving diameter will be improved. Figure 5 also indicates that the tendency in conditions of strong atmospheric turbulence is the same, but the influence of the DOEs on the BER is not so obvious. As we can see, at $D_r = 1.05$ m, introducing the DOEs can improve the BER by 10^{-1} under weak atmospheric turbulence while the improvement of the BER will only be $10^{-0.5}$ under strong atmospheric turbulence. The reason is obvious. It is because the average receiving power under strong atmospheric turbulence is smaller than that under weak atmospheric turbulence, which will decrease the function of the DOEs on the BER. In all, introducing the DOEs can help decrease the required receiving diameter at the same BER performance, which is helpful for the miniaturization of the satellite volume.

Corresponding to the receiving diameter at Rx, the transmitting aperture at Tx also influences the BER performance. However, the BER relationship curve versus the transmitting aperture is not monotonically increasing or decreasing. As it shows in Fig. 6, there exists a best transmitting aperture in each space optical communication system. According to Ref. [25], at a small transmitting aperture the transmission beam will be more influenced by beam wander, while at a large transmitting aperture the transmission beam will be influenced more by intensity

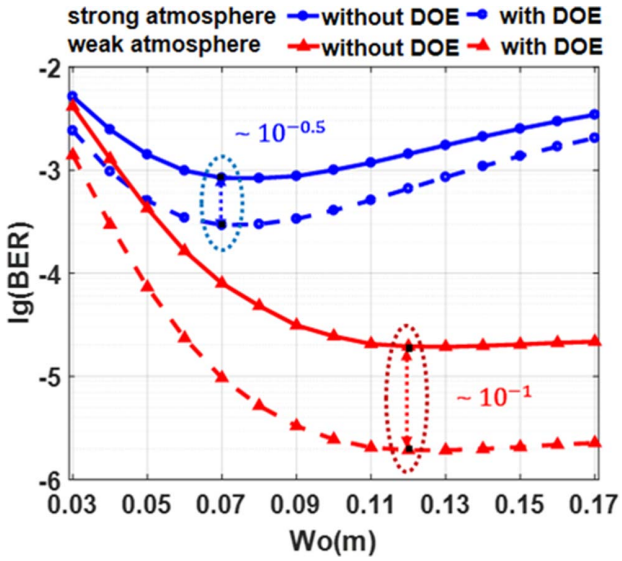

Fig. 6. BER relationship versus the transmitting aperture at different atmospheric turbulence conditions.

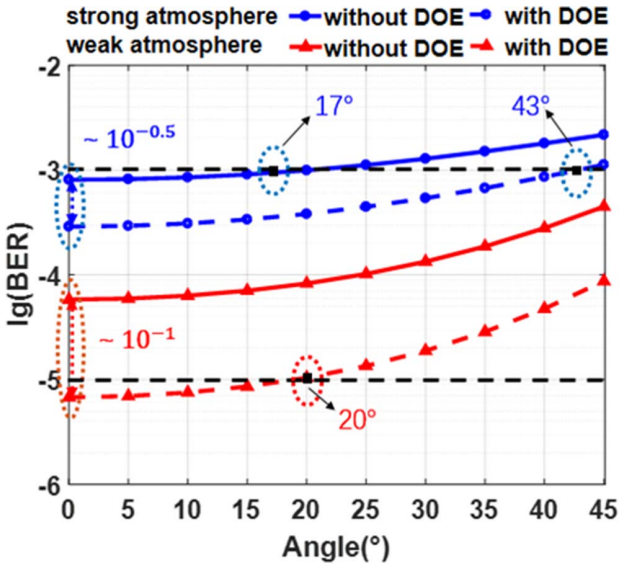

Fig. 7. BER relationship versus the zenith angle at different atmospheric turbulence conditions.

fluctuation. So the system can achieve a good BER performance only when the transmitting aperture is set to a proper value. We can also find that the best transmitting aperture under a strong atmospheric turbulence is around 0.07 m and the best transmitting aperture under a weak atmospheric turbulence is around 0.12 m. That is because the variation of the atmospheric refractive index coefficient C_n^2 changes both the intensity fluctuation effect and the beam wander effect. So, the best transmitting aperture under a strong atmospheric turbulence is different from that under a weak atmospheric turbulence. It should be noted that introducing the DOEs hardly influences the best transmission aperture, as the effects of atmospheric turbulence will not be obviously affected by the introduction of the DOEs. Also, we can find that the DOEs can decrease the BER efficiently and improve the communication quality. In this Letter, the DOEs can decrease the BER by around $10^{-0.5}$ and 10^{-1} at the best transmission aperture in strong and weak atmospheric turbulence conditions.

Zenith angle is another basic parameter at Tx. The ideal zenith angle is 0°, but for practical communication link requests the zenith angle is set according to the position of Tx and Rx. From Fig. 7 we can see that the DOEs can decrease the BER by around 10^{-1} and $10^{-0.5}$ at a zenith angle of 0° under weak and strong atmospheric turbulence, respectively. If the BER is aimed to be kept below 10^{-3} under strong atmospheric turbulence effects, introducing the DOEs can enlarge the range of the zenith angle from [0°–17°] to [0°–43°]. In case of weak atmospheric turbulence, the BER in the system without the DOEs is higher than 10^{-5} when the zenith angle is 0°. After introducing the DOEs, the BER can be kept below 10^{-5} with the range of zenith angle of [0°–20°]. In all, introducing the DOEs can allow a wider range of zenith angle, which greatly increases the flexibility of the practical system design.

Bit rate is another important measuring parameter in space optical communication systems as mass data need to be transferred. The BER relationship with bit rate under strong and weak atmospheric turbulences is shown in Fig. 8. The BER deteriorates with the increase of bit rate. Under weak atmospheric turbulence, introducing the DOEs can decrease the BER from around 10^{-9} to 10^{-11} at 0.1 Gbps and from around 10^{-4} to 10^{-5} at 1 Gbps. We can see that the influence of the DOEs on the BER decreases with the increase of bit rate. The effect of the DOEs on the BER under strong atmospheric turbulence is similar, but the overall effect of the DOEs on the BER is smaller than that under weak atmospheric turbulence. The results indicate that introducing the DOEs into the optical subsystem at Tx can decrease the BER,

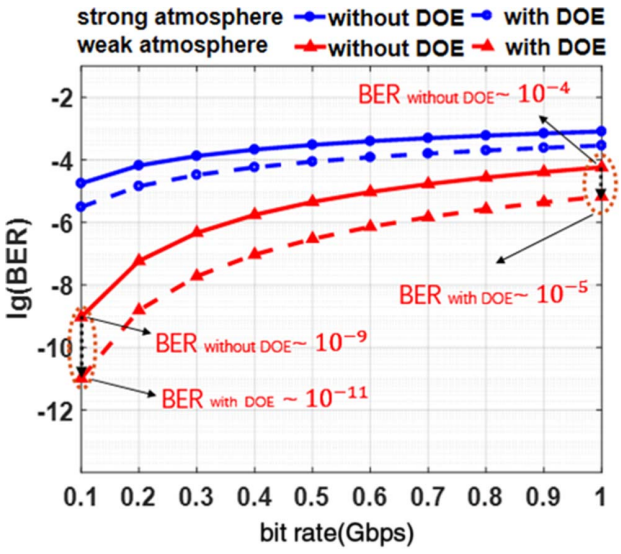

Fig. 8. BER relationship versus the bit rate at different atmospheric turbulence conditions.

which enables the space optical communication system with a higher bit rate. Thus, the space uplink chaotic optical communication system can achieve a better performance under a weak atmospheric turbulence.

In this Letter, we introduce a couple of DOEs at Tx to improve the communication quality of the MSK space uplink chaotic optical communication system. The DOEs realize the intensity re-distribution through changing the phase of each point of transmission spots. They will not influence the beam profile at the exiting pupil, so the far-field transmission process will not be affected for the use of the DOEs. The substantial effect of the DOEs is to complement the power lost during the beam expanding process at Tx. Then we build the BER model to discuss the effect of the DOEs on the communication performance and give the BER relationship curves versus basic system parameters. According to our simulation results, the DOEs perform well both under strong and weak atmospheric turbulences. Introducing the DOEs into the MSK space uplink chaotic optical communication system can help decrease the required transmission power or receiving diameter, allowing a wider zenith angle range and larger bit rate while the system maintains a good BER performance at the same time. Since the DOEs can be easily designed by computers, and introducing the DOEs into the chaotic space optical communication is not complex, introducing the DOEs into space uplink chaotic optical communication systems is of great value.

This work was supported by Joint Funds of Space Science and Technology (No. 6141B060307), Suzhou Technology Innovative for Key Industries Program of China (No. SYG201729), National Natural Science Foundation of China (No. 61205045), Fundamental Research Funds for the Central Universities (No. 021314380152), and Six Talent Peaks Project in Jiangsu Province (No. KTHY-003).

References

1. J. H. Ji, J. J. Zhang, B. Wu, K. Wang, and M. Xu, Chin. Opt. Lett. **17**, 080604 (2019).
2. S. Y. Fu, Y. W. Zhai, H. Zhou, J. Q. Zhang, C. Yin, and C. Q. Gao, Chin. Opt. Lett. **17**, 080602 (2019).
3. W. Zamrani, E. Ahouzi, A. Lizana, J. Campos, and M. J. Yzuel, Opt. Eng. **55**, 103108 (2016).
4. B. B. Wu and E. E. Narimanov, Opt. Express **14**, 3738 (2006).
5. J. M. Liu, H. F. Chen, and S. Tang, IEEE J. Quantum Electron. **38**, 1184 (2002).
6. A. Argyris, D. Syvridis, L. Larger, V. Annovazzi-Lodi, P. Colet, I. Fischer, J. García-Ojalvo, C. R. Mirasso, L. Pesquera, and K. A. Shore, Nature **438**, 343 (2005).
7. C. R. Mirasso, P. Colet, and P. García-Fernández, IEEE Photonics Technol. Lett. **8**, 299 (1996).
8. Y. Liu, Y. Takiguchi, and P. Davis, Appl. Phys. Lett. **80**, 4306 (2002).
9. N. F. Rulkov, M. A. Vorontsov, and L. Illing, Phys. Rev. Lett. **89**, 277905 (2002).
10. J. S. Hu, Z. C. Zhang, L. Wu, J. Dang, and G. H. Zhu, Chin. Opt. Lett. **16**, 120101 (2018).
11. A. Yamamoto, T. Hori, T. Shimizu, and K. Nakagawa, Proc. SPIE **2210**, 30 (1994).
12. H. Hemmati and N. Page, Proc. SPIE **3615**, 206 (1999).
13. M. Knapek, J. Horwath, N. Perlot, and B. Wilkerson, Proc. SPIE **6304**, 63041U (2006).
14. L. Y. Tan, J. J. Yu, J. Ma, Y. Q. Yang, M. Li, Y. J. Jiang, J. F. Liu, and Q. Q. Han, Opt. Express **17**, 6311 (2009).
15. Z. Liu, J. Dai, X. Sun, and S. Liu, Opt. Express **16**, 19926 (2008).
16. T. Heil, I. Fischer, and W. Elsäßer, Phys. Rev. Lett. **87**, 243901 (2001).
17. S. M. Redmond, D. J. Ripin, C. X. Yu, S. J. Augst, T. Y. Fan, P. A. Thielen, J. E. Rothenberg, and G. D. Goodno, Opt. Lett. **37**, 2832 (2012).
18. E. C. Cheung, J. G. Ho, G. D. Goodno, R. R. Rice, J. Rothenberg, P. Thielen, M. Weber, and M. Wickham, Opt. Lett. **33**, 354 (2008).
19. J. W. Goodman, *Introduction to Fourier Optics*, 3rd Edition (Roberts and Company Publishers, 2005).
20. J. J. Jones, *Modern Communication Principle with Application to Digital Signaling* (McGraw-Hill, 1967).
21. F. Dios, J. A. Rubio, A. Rodriguez, and A. Comeronn, Appl. Opt. **43**, 3866 (2004).
22. J. C. Ding, M. Li, M. H. Tang, Y. Li, and Y. J. Song, Opt. Lett. **38**, 3488 (2013).
23. M. Li, Y. F. Hong, Y. J. Song, and X. P. Zhang, Opt. Express **26**, 2954 (2018).
24. M. Li, B. W. Li, X. P. Zhang, Y. J. Song, L. Q. Chang, and Y. Chen, Opt. Commun. **366**, 248 (2016).
25. J. Ma, Y. J. Jiang, L. Y. Tan, S. Y. Yu, and W. H. Du, Opt. Lett. **33**, 2611 (2008).
26. H. Avetisyan and C. H. Monken, Opt. Express **24**, 2318 (2016).
27. Y. C. Kouomou, P. Colet, L. Larger, and N. Gastaud, IEEE J. Quantum Electron. **41**, 156 (2005).